Session 5

Solar Wind – Origin and Evolution

Courtesy National Museum Cairo. From Tell el-Amarna, 1400 B.C.

https://doi.org/10.1017/S1743921306001980 Published online by Cambridge University Press

Solar Activity and its Magnetic Origin
Proceedings IAU Symposium No. 233, 2006
V. Bothmer & A. A. Hady, eds.

doi:10.1017/S1743921306001980

Origin and evolution of the solar wind

E. Marsch[1]

[1]Max-Planck-Institut für Sonnensystemforschung, 37191 Katlenburg-Lindau, Germany
email: marsch@mps.mpg.de

Abstract. The magnetic field of the Sun and the plasma properties of its atmosphere, such as temperature, density and waves in the solar corona, determine the origin, energetics and evolution of the solar wind. The solar wind comes in three main kinds, as steady fast streams, variable slow flows and transient fast coronal mass ejections, with all being closely associated with the structure and activity of the coronal magnetic field that evolves on a multitude scales. This tutorial paper places emphasis on the observed and measured characteristics of the solar wind sources and their magnetic structure. The boundary conditions in the magnetically closed corona, in the transiently opening corona, and in the lastingly open corona (funnels and holes) will be discussed, and their influences on and consequences for the interplanetary solar wind be addressed. The resulting three-dimensional structure of the solar wind and its evolution over the solar cycle are also briefly discussed.

Keywords. Solar corona, magnetic field, solar wind, ultraviolet emission

1. Introduction

The solar wind is basically determined by the Sun's magnetic field and responds in various ways to solar activity and the accompanying changes in the photospheric magnetic field, which determines the coronal magnetic field and therewith the interplanetary magnetic field and solar-wind stream structure in the entire heliosphere. For a modern review of the solar magnetic field see Solanki *et al.* (2006). The sources of the solar wind are defined by the solar magnetic field, and the origin of the solar wind is closely linked with and influenced by the structure and activity of the magnetic network and the solar transition region (TR).

As the result of varying boundary conditions in the corona, three basic types of solar wind occur: Fast streams from large coronal holes (CHs); slow streams from small CHs and active regions (ARs), and from the boundary layers of coronal streamers; and the variable transient flows such as coronal mass ejections (CMEs), often associated with eruptive prominences, or plasmoids stemming from the top of streamers, and other ejections from ARs driven through magnetic flux emergence and reconnection. These basic types of solar wind (for recent reviews see, e.g., Marsch (2006) and Schwenn (2006)) are closely associated with the structure and the activity of the coronal magnetic field that changes over the solar cycle. CMEs as such and their interplanetary manifestations (see e.g. Bothmer & Schwenn (1998)) will not be discussed here.

This paper gives a concise review of the origin of the solar wind, with emphasis on the physical nature of the source regions, as they are evident in the solar extreme ultraviolet (EUV) emission patterns and in coronagraph images. The plasma characteristics as well as the magnetic structures of the solar wind source regions are reviewed in a tutorial fashion. The boundary conditions in the mostly closed corona (streamers and loops), in the transiently opening corona (eruptive prominences and flux tubes) and in the lastingly open corona (funnels and holes) will be briefly dicussed, in particular for small scales and from the observational point of view.

2. Basic properties of the solar wind

In this short section we will address the basic energetics of the solar wind, and list a few of its typical parameters. The energy flux density required at 1 R_S to drive the fast solar wind is $F_E = 5 \times 10^5$ erg cm^{-2} s^{-1}, the observed terminal speed beyond 10 R_S is $V_p = 700 - 800$ km s^{-1}, the remotely-inferred temperatures at 1.1 R_S are $T_e \approx T_p = 1 - 2 \times 10^6$ K, and the in-situ at 1 AU measured values are $T_p = 3 \times 10^5$ K, $T_\alpha \approx 10^6$ K, and $T_e = 1.5 \times 10^5$ K. The heavy-ion temperature is found to scale in proportion to their mass ratio with the proton temperature, i.e., $T_i \approx m_i/m_p T_p$, and the ion differential speed obeys the relation $\mathbf{V}_i - \mathbf{V}_p = \mathbf{V}_A$. Both phenomena that are still asking for a convincing theoretical explanation. For more details on the fluid and kinetic properties of the interplanetary solar wind plasma see the review paper of Marsch (1991).

The basic energy requirement on the solar wind acceleration can be derived from a Bernoulli-type energy equation, which compares the coronal enthalpy with the sum of the gravitational binding energy and asymptotic kinetic energy of a solar wind proton-electron pair,

$$\gamma/(\gamma - 1) 2 k_{\rm B} T_C = 1/2 m_p \big(V_\infty^2 + V_p^2\big). \tag{2.1}$$

Here the polytropic index is $\gamma = 5/3$, and the escape speed from the solar surface is $V_\infty = 618$ km s^{-1}. The effective coronal temperature T_C must be about 10^7 K, in order to obtain a wind flow speed of $V_p = 700$ km s^{-1} in the Earth orbit. This temperature is by an order of magnitude higher than typical observed values in the open corona, and therefore the necessary energy most likely comes from waves. The fluxes of energy and mass must be generated in, or continuously fed through, the magnetic network and then brought to the corona. The total energy required to sustain the fast solar wind corresponds for a proton-electron pair to a specific value of about 5 keV. For a more comprehensive discussion of solar wind models and theory see the reviews by Axford & McKenzie (1997) or Marsch *et al.* (2003), who also addresses aspects of kinetic solar wind theory and observations.

3. Coronal magnetic field

The coronal magnetic field has hardly ever been measured directly, but it can be obtained by force-free extrapolation techniques (for a summary of the state of the art in this field see, e.g., Wiegelmann & Neukirch (2002)). An example of the resulting model field of the active Sun is shown in Fig. 1, after Wiegelmann & Solanki (2004). An active region mainly consists of closed magnetic loops, in which dense plasma is confined, and therefore causes bright emission. In contrast, in CHs the large-scale magnetic field is open, and thus from them tenuous plasma can on open field lines freely escape in the form of the solar wind. Here the emission is strongly reduced as a result. This fact is obvious in any of the ultraviolet EIT coronal images, which regularly are obtained on SOHO and not reproduced here again.

The solar magnetic field determines the solar wind flow pattern and the structure of the corona. The coronal magnetic field gradually evolves with increasing distance from the Sun into the heliospheric (interplanetary) magnetic field. At some height, corresponding to the so-called source surface which is usually assumed to be located at 2.5 to 3 R_S, the field becomes frozen into the solar wind. The potential-field model extrapolates the magnetic field as being measured in the photosphere to the corona, while postulating that the coronal field is free of currents. The source surface is a virtual sphere from which on the outer coronal field is assumed to be radial. Thus the magnetic field polarity changes across the heliospheric current sheet (HCS), which is linked with the equatorial

https://doi.org/10.1017/S1743921306001980 Published online by Cambridge University Press

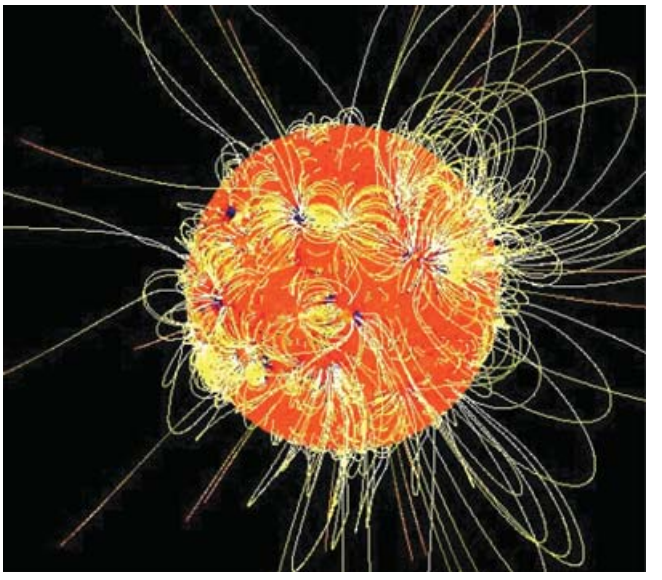

Figure 1. Coronal magnetic field as obtained by force-free extrapolation from photospheric magnetograms after Wiegelmann & Solanki (2004). The closed loops mostly correspond to bipolar active regions, or also may bridge widely separated regions of opposite polarity, whereas the open lines illustrate the coronal magnetic field that is open to the heliosphere and corresponds to the magnetic flux carried away by the solar wind (after Wiegelmann & Solanki (2004)).

streamer belt. During solar minimum the HCS extends as a symmetric disk far out into interplanetary space. Hoeksema (1995) has in detail described this model, and in particular the solar magnetic field and HCS as they evolved during the early Ulysses epoch over a full solar cycle. Marsch (2006) addressed the solar-wind responses to the Sun's changing magnetic activity.

The structure of the solar corona is simplest around minimum activity, where the field can be well modeled by a superposition of dipolar, quadrupolar, and current-sheet-related components after Banaszkiewicz *et al.* (1998). This minimum-type corona is shown in Fig 2. The related three-dimensional structure of the solar wind was only fully revealed by the Ulysses mission. In a grand overview plot, McComas *et al.* (2003) have illustrated the global structure of the solar wind and its variation over the solar cycle. Over the poles, high-speed solar wind originating in the polar CHs prevails in solar minimum, whereas slow wind coming from the streamer belt then dominates at low latitudes. The magnetic field becomes multipolar towards solar maximum activity, and the solar wind source regions accordingly change in locations and spatial extents. Similarly, the solar wind flow pattern becomes more complex and variable.

The changing solar corona and associated solar wind are shown in Fig. 3, which reproduces the general survey plot of McComas *et al.* (2000) and gives a sequence of coronal images in the top panel and the solar wind speed in the bottom panel versus time and heliographic latitude. The transition from the minimum-type corona around 1995 to a maximum-type near 1999 is obvious and accompanied with a striking transition from steady fast to variable slow solar wind. The recurrent-stream oscillations between 1996 and 1997 were due to solar rotation that caused rapid transitions of the spacecraft into and out of the HCS, respectively the open field related to the polar CHs, and thus resulted in a periodic variation between fast and slow flows. At the bottom of the panel, the occurrence times of CMEs are also indicated.

https://doi.org/10.1017/S1743921306001980 Published online by Cambridge University Press

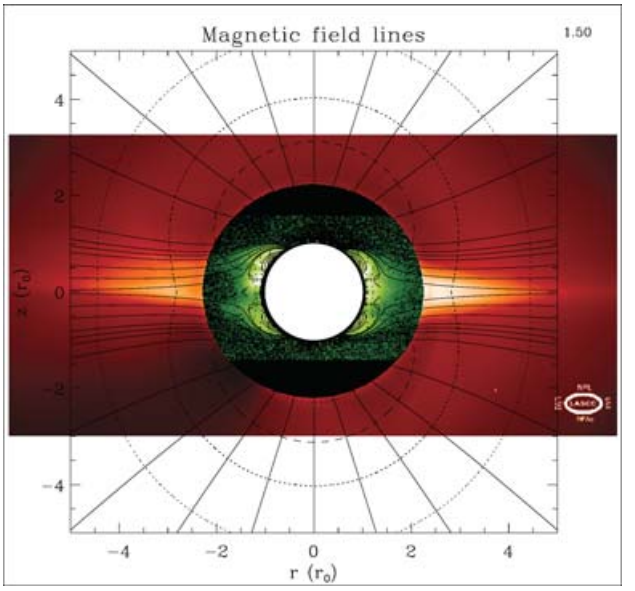

Figure 2. The highly symmetric solar corona at minimum activity and the associated coronal model magnetic field. Superposed coronal images from EIT and LASCO (green corona line) indicate the large dark polar CHs and the low-latitude current sheet coinciding with the small bright streamer belt (after Forsyth & Marsch (1999)).

In addition to the steady streams, CMEs represent the other basic type of (variable and sporadic) solar wind (or solar better storms). For short introduction to this subject we refer to the tutorial paper of Srivastava & Schwenn (2000). Concerning their ocurrence rate, the CMEs tend to accumulate around maximum solar activity, when the corona is highly magnetically structured and of multi-polar nature. They seem to come in two main types, as slow and fast CMEs, although this classification is not unique. A sizable fraction (about 30%) of CMEs have, after Tripathi *et al.* (2004), large eruptive prominences at their origin, the remnants of which can be observed as post-eruptive arcades.

For CMEs the energy requirements and acceleration mechanisms are much less understood than for the steady streams. The recent review by Zhang & Low (2005) emphasizes the hydromagnetic nature of CMEs, provides a list of the relevant theoretical literature and gives a summary of the basic theory and model ideas. The paper by St. Cyr *et al.* (2004) reviews for the past ten years the space observations from SOHO and the characteristics of CMEs. The constraints on the plasma are even more extereme for a transient CME than for a steady solar wind stream, as the CME plasma density is often much higher, and its flow speed may easily reach a multiple of the average solar-wind speed.

4. Source regions of the solar wind

Whereas the global association of fast wind with large CHs and of slow wind with the streamer belt (see e.g. Sheeley *et al.* (1997)) and small CHs is long well established, the tracing of the in-situ observed solar wind to its sources at smaller scales on the Sun is not an easy task. In this section we will present some results in which the sources were identified through a combined analysis of Doppler shifts and radiances of ultraviolet emission lines together with the coronal magnetic field, as it was obtained by the extrapolation from a magnetogram measured in the solar photosphere.

https://doi.org/10.1017/S1743921306001980 Published online by Cambridge University Press

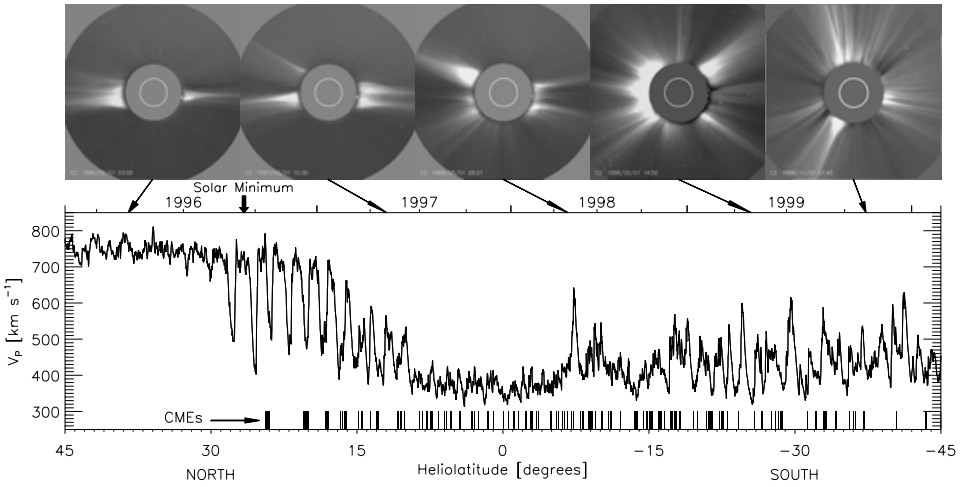

Figure 3. The changes of the solar corona (top) over the solar cycle and the corresponding variations in the solar wind flow pattern as a function of time or heliographic latitude along the Ulysses spacecraft orbit. Note the recurrent streams after mimum. The occurrence of CMEs is marked by the small vertical bars attached to the bottom scale (after McComas *et al.* (2000)).

The steady solar wind consists of two major components: fast, tenuous, and uniform flows from large CHs, and slow, dense, and variable flows from small CHs, often from near the boundaries between closed and open coronal fields. There are various techniques of mapping such flows back to the Sun in order to identify their sources in the corona. Whereas the origin of fast streams seems clear, the sources of the slow solar wind remain less obvious. Recently, Arge *et al.* (2003) for example studied what appeared to be narrow CHs in the Yohkoh soft X-ray images, and identified them to be the sources of slow solar wind, which also revealed large magnetic-field expansion factors. Similarly, Ohmi *et al.* (2003) by using WIND spacecraft data found that slow streams can emanate from small CHs in the vicinity of ARs.

4.1. *Solar wind from funnels in coronal holes*

The detailed source regions of the fast solar wind were recently found by Tu *et al.* (2005a) to be identical with the so-called coronal funnels in a CH, i.e. expanding magnetic field structures rooted in the magnetic network lanes. These authors corroborated and complemented the earlier work of Hassler *et al.* (1999), and established that the solar wind starts flowing out of the corona at heights above the photosphere between 5 Mm and 20 Mm in the funnels. This result was obtained by a correlation of the Doppler-velocity and radiance maps of different spectral lines. Specifically, Ne^{7+} ions were found to mostly radiate around 20 Mm, where they have outflow speeds of about 10 km s^{-1}, whereas C^{3+} ions with no average flow speed mainly radiate around 5 Mm. These new findings are illustrated in Fig. 4, which shows in three planes at heights of 0, 4 and 20 Mm the color-coded maps of the magnetic field strength. Regions with outflow speed larger than 7 km s^{-1} are indicated in the top plane by the hatched patches that coincide with the open, unipolar and strong magnetic field representing the funnels.

Stimulated by these observations, a new model was suggested to explain the origin of the fast solar wind. The transition region (TR) in CHs is full of magnetic loops of different sizes, mostly with a height of less than 5 Mm. The supergranular convection in the photosphere keeps the feet of the loops moving and thus transfers kinetic energy to

https://doi.org/10.1017/S1743921306001980 Published online by Cambridge University Press

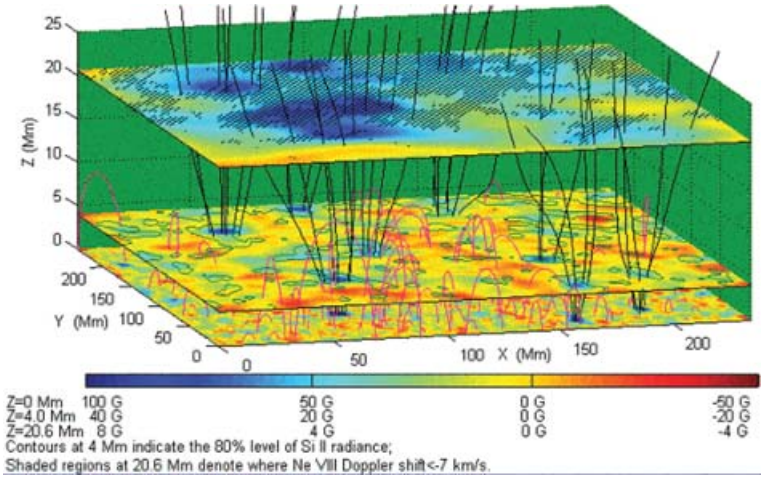

Figure 4. Source of the fast solar wind in magnetic funnels of a CH. The magnetic field magnitude is shown in two planes at 4 Mm and 20 Mm. The hatched areas indicate outflow speeds of neon ions larger than 7 km s^{-1}. The open field is indicated by black lines, and the closed loops in magenta color. They hardly reach a height of 10 Mm (after Tu *et al.* (2005a)).

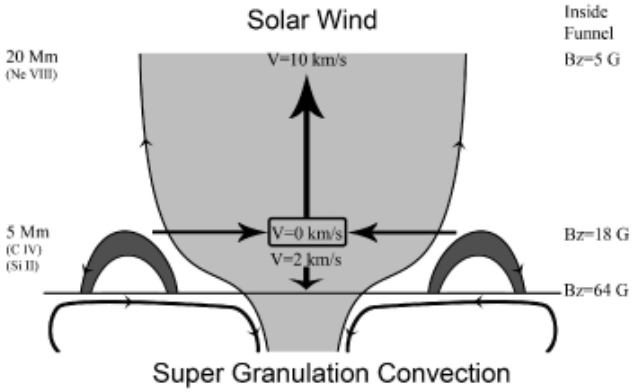

Figure 5. Source region of the fast solar wind in a magnetic funnel of a CH. This sketch illustrates the scenario of the solar wind origin and its energy and mass supply, mainly through the side loops. Ultimately, magnetoconvection is the driver of solar wind outflow in coronal funnels. Thus mass and also wave energy are delivered to the funnel by magnetic reconnection. Funnel and loops are drawn according to their real scale sizes (after Tu *et al.* (2006)).

magnetic energy that is stored in the loops. They may finally collide with the funnel and there reconnect the with pre-existing open field. Plasma of the loops is thus released, and may lead to both upflows and downflows. Ultimately, parts of the plasma contained in reconnecting loops are brought into the corona. In the lower TR below about 5 Mm, we mainly have horizontal exchange of mass and energy between neighboring flux tubes, which is driven by supergranular motion. Above 5 Mm or higher, where reconnection between field lines of funnels and surrounding loops gradually ceases, vertical transport will become more important than horizontal, and the radial acceleration of the solar wind will actually start. This scenario after Tu *et al.* (2006) is illustrated in Fig. 5. It is a further development of the magnetic furnace idea of Axford & McKenzie (1997).

https://doi.org/10.1017/S1743921306001980 Published online by Cambridge University Press

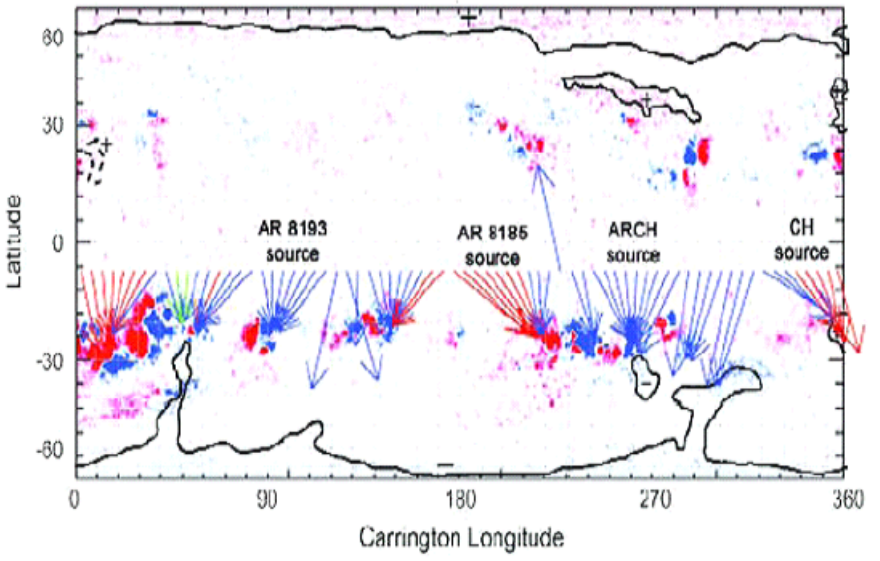

Figure 6. Source regions of the solar wind, which is found to originate in active regions and small CHs. The arrows indicate the mapping of open flux from the source surface (at 2.5 R_S) back to the photosphere. Red (blue) means inward (outward) magnetic polarity, and the green lines lie near the current sheet (after Liewer *et al.* (2003)).

4.2. *Solar wind from active regions*

It is only recently, that ARs near solar maximum were clearly identified as the source regions of slow solar wind. For example, Liewer *et al.* (2003) investigated the magnetic topology of several ARs in connection with EUV and X-ray images. Synoptic coronal maps were employed for mapping the inferred sources of the solar wind from the magnetic source surface down to the photosphere. In most cases, a dark lane, as it is familiar for the small CHs, was seen in the EUV images, thus suggesting an open magnetic field. They studied in particular a magnetogram for AR 1934 and used a magnetic field extrapolation model, thus mapping the open flux from the source surface at 2.5 R_S down to the photosphere. Thus several different sources (ARs and CHs) became clearly evident. They are shown in Fig. 6 which was taken from Liewer *et al.* (2003). In their synoptic map the arrows indicate the mapping of the solar wind from the source surface (arrow tails) to the photosphere (arrow heads). The in-situ composition data of the solar wind associated with these regions indicates high freezing-in temperatures of the heavy ions, a result that is consistent with the inference that the AR indeed is a genuine source of the solar wind.

Marsch *et al.* (2004) also studied ARs in connection with coronal the magnetic field as obtained by extrapolation and together with EUV Doppler shifts and images. They could establish that the dark (in ultraviolet emission) areas adjacent to the closed AR loops can indeed be magnetically open, and apparently reveal strong upflows in hot coronal emission lines. An example is given in Fig. 7, where on the left side the magnetic field of AR 7953 associated with a sunspot is shown, as obtained by force-free field extrapolation (see the review of Wiegelmann and Neukirch, 2002), and on the right side the Doppler-shift pattern indicating strong local plasma flows in the coronal loops of the AR. In the sunspot, the material clearly streams upward with a speed of several 10 km s^{-1}, whereas the adjacent closed loops are mostly related to downflows. Whether the upflow actually

https://doi.org/10.1017/S1743921306001980 Published online by Cambridge University Press

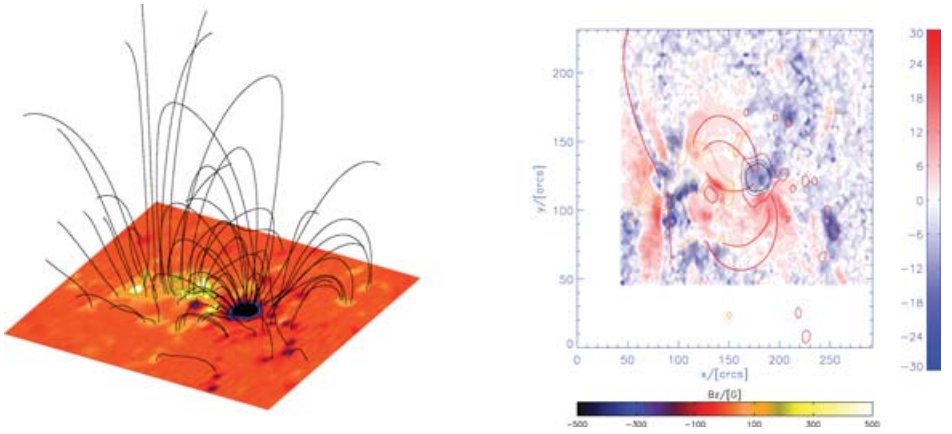

Figure 7. Left: Coronal magnetic field topology in three dimensions for the bipolar AR 7953. Field lines above the solar surface with $B_z > 50$ G on the photosphere are plotted. The color coding represents the magnetic field strength. Right: SUMER Dopplergram in Ne VIII (77 nm) and a 2-D-projection of selected reconstructed field lines, as obtained from a force-free-field extrapolation with the model parameter $\alpha = -1.1 \times 10^{-8}$ m^{-1}. Additional colored contours of the magnetic field strength on the photosphere are also shown. Note the sizable plasma flows, reaching speeds of 25 km s^{-1} in the corona, with significant outflow in the sunspot at the center of the AR (after Marsch *et al.* (2004)).

continues into the upper corona for this AR remains unclear, but it appears to be likely according to the results shown in Fig. 7.

In conclusion, solar wind at times comes from the active Sun, i.e. from ARs and their small neighbouring CHs. How many of such regions during solar maximum are associated with slow solar wind remains to be investigated. The question is still open if solar wind can also originate in the quiet corona, which mainly consists of closed magnetic loops of different sizes.

4.3. *Solar wind from the quiet sun?*

From correlations between the radiance of solar ultraviolet emission and the vertical magnetic field component, as obtained by extrapolation from photospheric magnetograms to different heights, one can determine the correlation height of the emission source, by identifying the altitude at which the correlation coefficient has its maximum. In this way Tu *et al.* (2005b) found that for a quiet-Sun region the correlation height for Si II was near 2.1 Mm, C IV at 1.4 Mm, and Ne VIII at 3.7 Mm. The thickness of the TR was thus determined to be only about 2 Mm. The height profiles are illustrated in Fig. 8, which also shows on the left the related magnetic-field map at 2.1 Mm, with superimposed contours of the silicon-line radiance which coincide with regions of strong magnetic field.

A comparison between the extrapolated field lines and the Dopplershifts of Ne VIII indicates that weak blueshifts of 5 km s^{-1} occur in a few small regions with strong magnetic fields. Some of the closed field lines may reach as high as 10 Mm. Weak blueshifts do appear on both closed bi-polar regions and open unipolar regions. The low TR appears to be highly structured by a carpet of magnetic loops of different sizes. Most of the ultraviolet radiation is certainly coming from these loops. However, it remains unclear

https://doi.org/10.1017/S1743921306001980 Published online by Cambridge University Press

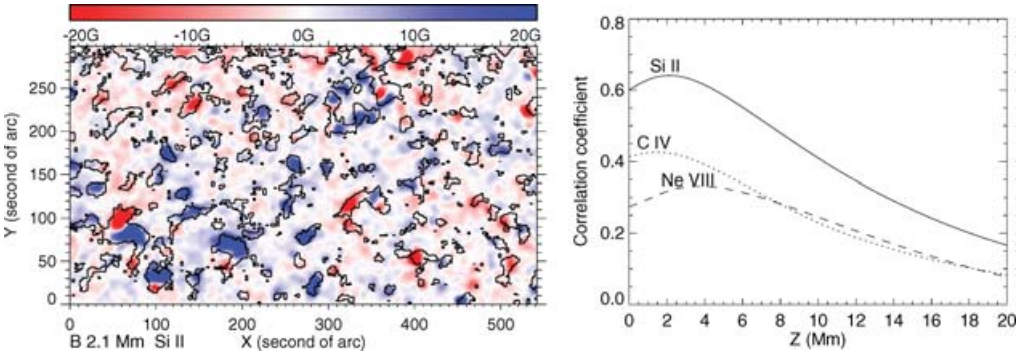

Figure 8. Left: Magnetic field intensity color-coded with superimposed contours of the SiII radiance for a quiet-sun region of the lower solar corona. Note the clear correlation between field strength and line intensity. Right: Correlation heights defining the mean altitude of the emission region for three ultraviolet lines. The TR height is about 2 Mm (after Tu *et al.* (2005b).

how much open magnetic flux may exist in between such closed loops in the quiet corona, and how the slow solar wind could originate from there.

5. Summary

We briefly reviewed the coronal origin of the solar wind and the sources of the fast and slow streams. Obviously, the magnetic field is the main player in the relevant physical processes, since it shapes the solar corona and thus defines the properties and dynamics of the nascent solar wind. The field topology and activity are the keys to understand how the solar wind originates in the corona. Since the unsigned radial magnetic flux at 1 AU is measured to be almost constant over the full sphere and at any time, there must be a constant fraction of open magnetic flux in the lower corona at any time of the solar cycle. As the Sun's magnetic field varies systematically over the solar cycle, from a simple dipolar structure (in minimum) to a complex multipolar structure (in maximum), so do the solar wind sources, and correspondingly varies the solar wind itself. Its plasma and energy have continuously to be supplied through the magnetic network into the TR and lower corona. Reconnection in the network appears to play a main role in the supply of mass and energy to the corona. In summary we may say that:

- The coronal magnetic field at all scales determines the solar origin and evolution of the solar wind.
- The solar wind comes in three types, as steady fast streams, variable slow flows and transient CMEs.
- The fast streams in minimum appear to originate in the funnels of the polar coronal holes, and in other phases of the activity cycle also from the low-latitude equatorial CHs.
- The slow streams in minimum come from streamers and their boundaries, whereas in solar maximum they can also originate in small CHs and near ARs.

The steady fast solar wind appears to originate in the rapidly expanding funnels (unipolar) in CHs, and some slow wind may as well be generated in such narrow unipolar open, or transiently open, funnels between myriads of dynamic loops in the quiet sun. Yet, there remain basic questions as to the origin of the slow wind. As measured in situ, it appears to be intrinsically variable, a property that most likely reflects the spatial and temporal variability of its coronal sources.

https://doi.org/10.1017/S1743921306001980 Published online by Cambridge University Press

References

Arge, C.N., Harvey, K.L., Hudson, H.S. & Kahler, S.W. 2003, in: M. Velli, R. Bruno & F. Malara (eds.), *Solar Wind Ten*, AIP Conf. Proc., Vol. 679, Melville, New York, USA, p. 202

Axford, W.I. & McKenzie, J.F. 1997, in: J.R. Jokipii, C.P. Sonett & M.S. Giampapa (eds.), *Cosmic Winds and the Heliosphere*, Arizona University Press, Tucson, pp. 31–66

Banaszkiewicz, M., Axford, W.I., & McKenzie, J.F. 1998, *Astron. Astrophys.* 337, 940

Bothmer, V. & Schwenn, R. 1998, *Ann. Geophysicae* 16, 1

Forsyth, R. & Marsch, E. 1999, *Space Sci. Rev.* 89, 7

Hassler, D.A., Hassler, D.M., Dammasch, I.E., Lemaire, P., *et al.* 1999, *Science* 283, 810

Hoeksema, J.T. 1995, *Space Sci. Rev.* 137

Liewer, C.P., Neugebauer, M. & Zurbuchen, T. 2003, in: M. Velli, R. Bruno & F. Malara (eds.), *Solar Wind Ten*, AIP Conf. Proc., Vol. 679, Melville, New York, USA, p. 51

McComas, D.J., Gosling, J.T. & Skoug, R.M. 2000, *Geophys. Res. Lett.* 27, 2437

McComas, D.J., Elliott, H.A., Schwadron, N.A., Gosling, J.T., Skoug, R.M. & Goldstein, B.E. 2003, *Geophys. Res. Lett.* 30, 1517

Marsch, E. 1991, in: R. Schwenn & E. Marsch (eds.), *Physics of the Inner Heliosphere*, Vol. 2, Springer Verlag, Heidelberg, pp. 45–133

Marsch, E., Axford, W.I. & McKenzie, J.F. 2003, in: B.N. Dwivedi (ed.), *Dynamic Sun*, Cambridge University Press, Cambridge, U.K., p. 374

Marsch, E., Wiegelmann, T. & Xia, L.D. 2004, *Astron. Astrophys.* 428, 629

Marsch, E. 2006, *Adv. Space Res.*, in press

Ohmi, T., Kojima, M., Hayashi K. *et al.* 2003, in: M. Velli, R. Bruno & F. Malara (eds.), *Solar Wind Ten*, IP Conf. Proc., Vol. 679, Melville, New York, USA, p. 137

Schwenn, R. 2006, *Space Sci. Rev.*, in press

Sheeley, N.R., Wang, Y.-M., Hawley, S.H. *et al.* 1997, *Astrophys. J.* 484, 472

Solanki, S.K., Schüssler, M. & Inhester, B. 2006, *Rep. Prog. Phys.* 69, 563

Srivastava, N. & Schwenn, R. 2000, in: K. Scherer, H. Fichtner & E. Marsch (eds.), *The Outer Heliosphere: Beyond The Planets*, Copernicus Gesellschaft e.V., Katlenburg-Lindau, Germany, pp 13–40

St.Cyr, O.C., Plunkett, S.P., Michels, D.J. *et al.* 2004, *J. Geophys. Res.* 105, 18169

Tripathi, D., Bothmer, V. & Cremades, H. 2004, *Astrophys. J.* 422, 337

Wiegelmann, T. & Neukirch, T. 2002, *Sol. Phys.* 208, 233

Wiegelmann, T. & Solanki, S.K. 2004, in: *Proc. the SOHO 15 Workshop – Coronal Heating*, St. Andrews, Scotland, 6-9 September 2004, ESA SP 2004

Tu, C.-Y., Zhou, C., Marsch, E., Xia, L.-D., Zhao, L., Wang, J.-X. & Wilhelm, K. 2005a, *Science* 308, 519

Tu, C.-Y., Zhou, C., Marsch, E., Wilhelm, K., Zhao, L., Xia, L.-D. & Wang, J.-X. 2005b, *Astrophys. J.* 624, L133

Tu, C.-Y., Zhou, C., Marsch, E., Wilhelm, K., Xia, L.-D., Zhao, L. & Wang, J.-X 2006, in: *Solar Wind Eleven*, in press

Zhang, M. & Low, B.C. 2005, *Annual Rev. Astron. Astrophys.* 43, 103